Collapse processes in abandoned pillar and stall coal mines: implications for shallow mine geothermal energy.

Billy J. Andrews[1*], Zoë A. Cumberpatch[2], Zoe K. Shipton[1], Richard Lord[1]

1) Department of Civil and Environmental Engineering, University of Strathclyde, Glasgow, G11XJ.
2) Department of Earth and Environmental Sciences, University of Manchester, Manchester, M13 9QQ.

Correspondence to: Billy J. Andrews (billy.andrews@strath.ac.uk)

Abstract. Flooded mine workings represent potential aquifers for shallow geothermal development projects. However, determining the collapse state of such workings in advance of drilling, and predicting their hydrogeological properties can be challenging, therefore developing an understanding of the products of mine collapse is important. We investigate the internal structure of collapsed pillar and stall mine workings exposed through coastal erosion near Whitley Bay, NE England. Our data suggests these workings collapsed in stages, leaving a clay-rich anthropogenic sedimentary layer consisting of collapse breccias and muds that will have gradually reduced the water capacity of the mine workings as collapse proceeded.

1. Introduction

The importance of coal during the industrial revolution and the large workforce required for its sub-surface extraction led to the development of densely populated areas underlain by a labyrinth of mine workings. Following the decline of sub-surface extraction, groundwater returns to pre-mining levels flooding the mine workings (Younger et al., 2002). These workings provide potentially large aquifers (e.g. a single coal seam in Pennsylvania and surrounding states contains $5.1 \times 10^{12} L$ of water (Watzlaf and Ackman, 2006)) that can be tapped to extract low-enthalpy geothermal heat using ground source heat pumps (Dochartaigh, 2009; Malolepszy et al., 2005; Monaghan et al., 2017). Additionally mine voids can be used for Aquifer Thermal Energy Storage (ATES) to store waste heat (e.g. waste industrial heat, refrigeration, air conditioning) for extraction when required (Hamm and Sabet, 2010; Patsa et al., 2015; Sanner, 2001). Heat pumps tapping flooded mine waters have significant potential in the decarbonisation and regeneration of densely populated ex-coal mining areas (Hamm and Sabet, 2010; Malolepszy, 2003; Malolepszy et al., 2005).

Sealed open loop systems are typically employed for mine water geothermal systems, with coupled extraction and injection wells (Banks et al., 2019). The volume of water which can be extracted from the mine reservoir, known as the water capacity (Lund, 2001; Loredo et al., 2017; Menéndez et al., 2019) should be high, though to avoid thermal breakthrough there should not be a direct connection between injection and extraction boreholes (Banks et al 2019). The up-front capital investment required in drilling is high, consequently it is desirable to be able to constrain the bulk hydrogeological properties of a mine before drilling.

While the methods of coal extraction varied through time (e.g. bell pits, shortwall, longwall), the pillar and stall method was widely used in the UK between the middle of the 14th and early 20th century (Fig. 1, Table 1) (Bruyn and Bell, 1999). Using this method coal was extracted from 'stalls', or 'rooms', supported by pit-props (Daunton, 1981), stacks and pillars wherein, 30 to 70% of the coal remained unworked to support the roof (Fig. 1) (Garrard and Taylor, 1988; Wardell and Wood, 1965). For mine geothermal prospects, the majority of flow will occur through open stalls (or their relicts), which will have very high permeability (Loredo et al., 2017). Rock pillars and temporary supports (e.g. pit props, colliery arches) were designed to sustain the weight of the overburden, however, following mining operations local stresses, rotting timbers, and the spalling of the pillars, can cause the roof to fail and eventually collapse (Bruyn and Bell, 1999; Helm et al., 2013; Lokhande et al., 2005). The failure of a single pillar will cause other pillars, particularly those in an up-dip direction, to become increasingly stressed and risk collapse causing a knock-on effect until the support of the overburden is significantly reduced (Bruyn and Bell, 1999). As roof material falls, the stalls become clogged and deformation migrates upwards in a predictable manner (e.g. Garrard & Taylor 1988; Madden and Hardmam, 1992), sometimes forming crown holes at the surface, depending on the thickness and lithology of the overburden. Pillar collapse and roof spalling, which can occur many years after mining operations have ceased (Carter *et al.* 1981; Salmi *et al.* 2019a, b) can lead to widespread subsidence (Gee et al., 2017) often occurring as individual collapse events over relatively short time scales (days to weeks) (Carter et al., 1981; Marino and Gamble, 1986).

While the structure above collapsed pillar and stall workings has been studied by many authors (e.g. Garrard and Taylor, 1988; Helm et al., 2013), particularly to understand mine-induced subsidence, the lithologies which make up the collapsed section and the processes by which they are deposited has received little attention. With the emergence of shallow mine geothermal prospects it is now important to understand the characteristics of these

55 ‘mine wastes’, and the processes involved if we are to improve our estimations of the water capacity and flow
56 properties of former pillar and stall workings. To address this we investigate exposures of workings near Whitley
57 Bay that have been exhumed by costal erosion. We use a detailed sedimentological approach and discuss the
58 implications of our findings for shallow mine geothermal projects targeting pillar and stall workings.

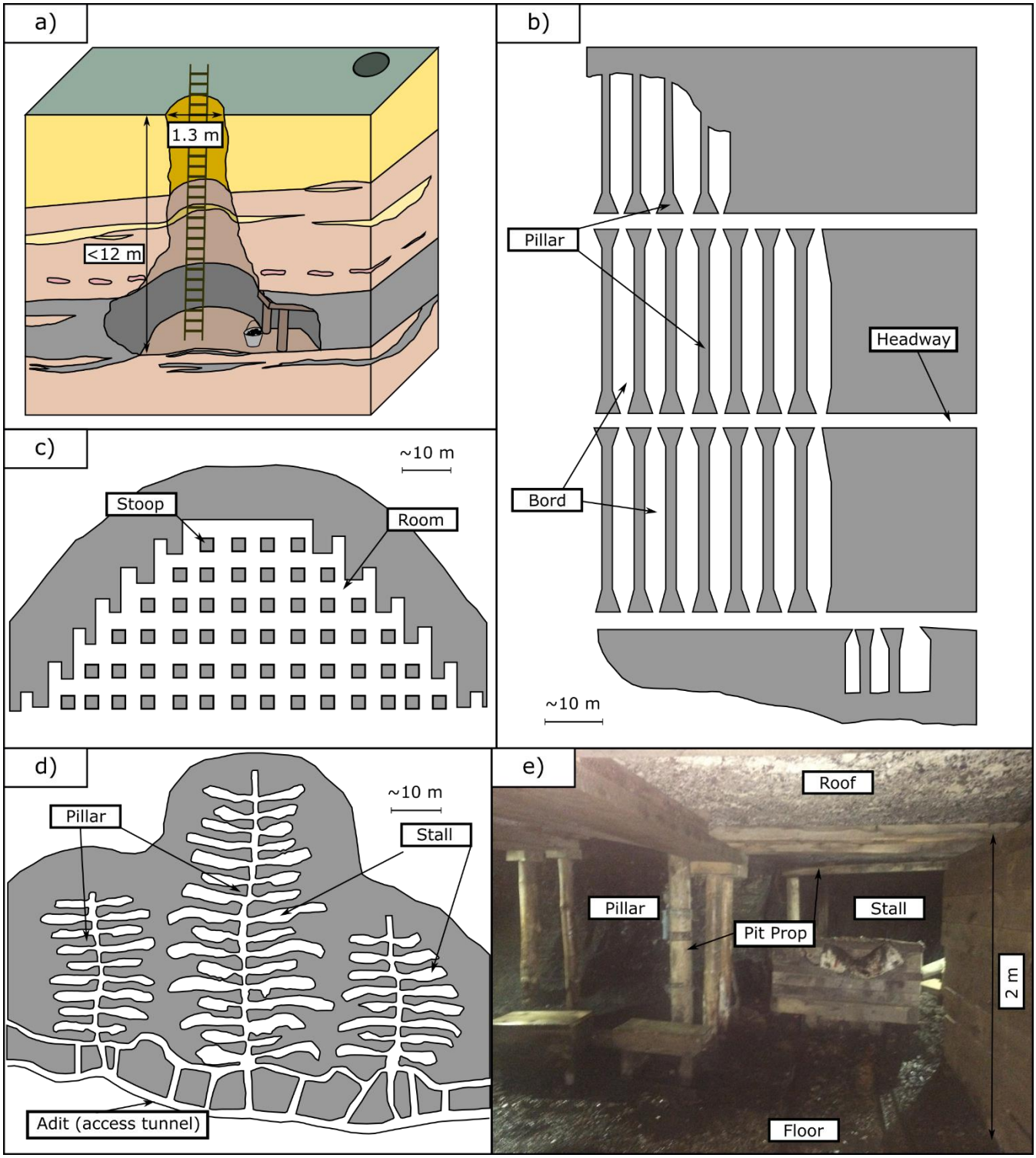

Figure 1: Typical UK shallow mining methods. (b) to (d) plan view pillar and stall mining methods to show regional variations in terminology and layout. (b, c and d redrawn from Bruyn and Bell (1999) a) bell pit, b) Bord-and-pillar workings, Newcastle upon Tyne (17th Century), c) Stoop and room workings, Scotland (17th Century), d) Pillar and stall workings, South Wales (17th Century), e) Photograph of pillar and stall workings, Beamish open air museum.

2. Geological history

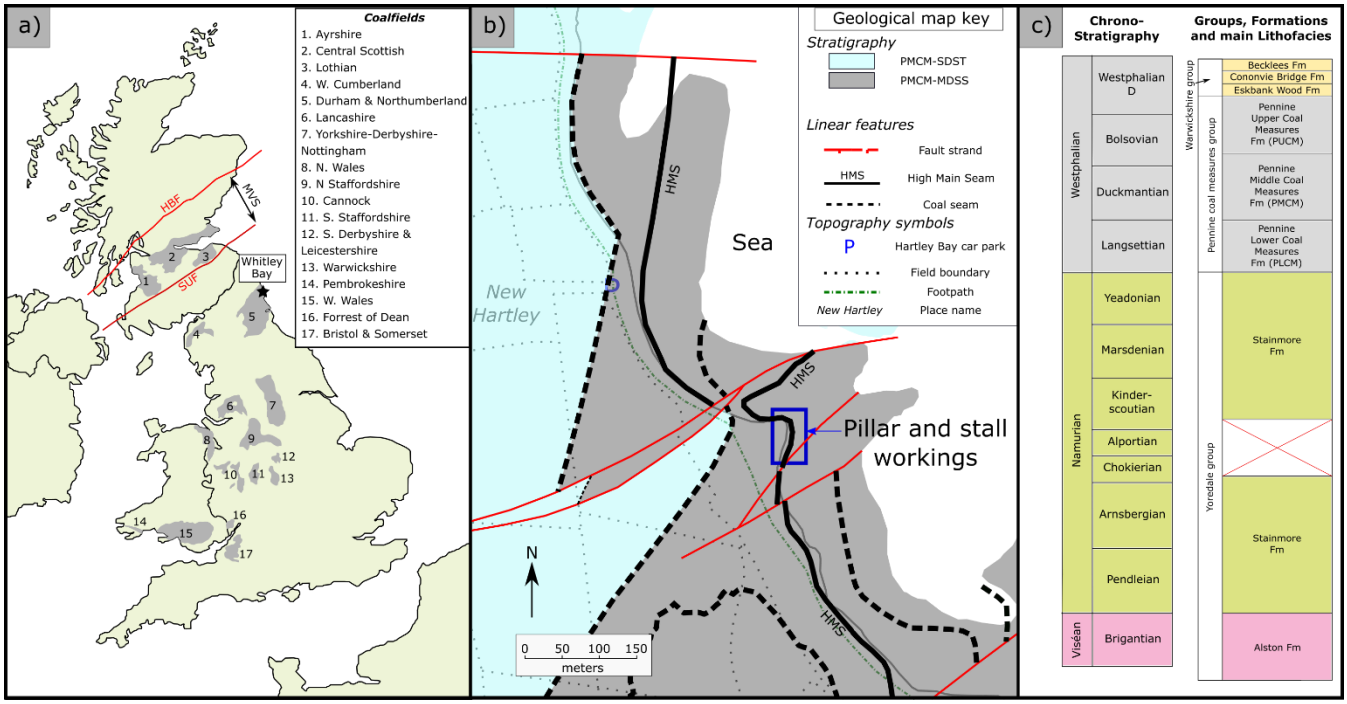

Figure 2: Geological setting. a) location of field site and UK coal fields (after (Donnelly et al., 2008), b) geology surrounding the workings near Whitley Bay, Northumberland (The map is modified from Geological Map Data BGS©UKRI (2018)) PMCM-SDST, c) Chrono-stratigraphy, formations and lithofacies of the Northumberland Trough (Chadwick et al., 1995). SDST = stand stone dominant sequence, MDSS = mudstone dominant sequence.

UK coal mine workings are found within mid-late Carboniferous sequences deposited in late Devonian-Carboniferous basins (Fig 2a). Coastal erosion has exposed a series of abandoned underground workings on the headland (National Grid square NZ34 76) just north of St Mary's Lighthouse, Whitley Bay (England) (Fig. 2b). Whitley Bay is located in the Northumberland Trough, a 50 km wide, ENE-WSW trending, half graben which formed in response to the extensional reactivation of the Iapetus Suture during the mid to late Carboniferous (Chadwick et al., 1995; Chadwick and Holliday, 1991; Johnson, 1984). The thickest coal seams (>2 m), many of which are workable; (Fielding, 1982; Smails, 1935), are almost exclusively confined to the Pennine Middle Coal Measures which reach 450 m thick in places (Fielding, 1984a; Leeder, 1974; Smails, 1935) (Fig. 2c).

Carboniferous lithologies at Whitley Bay consist of fossiliferous and barren mudstones (50 to 55%), siltstones and sandstones (40 to 48%) and bituminous coals (<5%), which nearly always occur above seat-earths (Fielding, 1984b; 1985, 1982; Jackson et al., 1985; Lawrence and Jackson, 1986). These are interpreted as being deposited on a broad, flat deltaic plain with numerous distributary channels (Fielding, 1984b; Fielding, 1985; Jackson et al., 1985). Exceptional exposures of the Pennine Middle Coal Measures, including the High Main Seam (HMS), are

observed along the 1.2 km long studied section (British National Grid NZ 364 756; Figure 2b), which dips gently E in low cliffs and rocky foreshore exposures.

The High Main Seam is highly variable in thickness (average 2 m, Fielding, 1982) and quality (Fielding, 1984a; Jackson et al., 1985; Lawrence and Jackson, 1986; Murchison and Pearson, 2000) with centimetre-to metre-scale shale partings commonly present (Fielding, 1982). Immediately below the HMS thin 'stringers' of coal (centimetre scale) are often found, which are locally workable (Fielding, 1982). Based on the history of the coalfield (Table 1), and because the workings are above the water table, we suggest the coal near Whitley Bay was extracted somewhere between 1550 and 1710 AD.

Date	UK wide	Northumberland and Durham Coalfields
Pre-1200	Extracted by shallow pits or adits (shallowly dipping tunnels)[1,2].	Workings of the High Main Seam date from Roman times[8].
1200s	Widespread coal mining began increasing up to, including and following the Industrial revolution.	Early shallow workings (<7 to 10 m) primarily using adits from the coast/valley side, with bell pits also used[9]
1300s	Bell-pits (Fig. 1a) became widespread[2,3].	
1500s	Most shallow reserves accessible by surface access methods extracted. The Pillar and Stall method began to be used[2,3] (Fig. 1d).	1550's saw the increased extraction of the HMS, with coal becoming a significant commercial interest[3,10,11,12]. Pillar and stall workings began in the late 16th Century[2].
1600s		The majority of coal close to sea-ports and above the water table extracted by the late 17th Century[13].
1700s		Technological advances in 1710 enabled coal to be mined below the water table[13].
1800's	Mining methods became standardised[1,2] (Fig. 1b, c & e). In 1850 detailed coal mine surveys began, with abandonment plans becoming mandatory from 1872[1,4].	1800 map of sea-sale collieries (where coal was shipped from local ports (e.g. the Port of Tyne)) does not include the workings near Whitley Bay[3]. 1830's to 1870s saw many large collieries opened up working the High Main Seam (e.g. Fenwick).
1900's	Many collieries switched to the use of longwall methods, with workings reaching depths in excess of 1 km (e.g. collieries near Glasgow).	1993: Easington colliery closes marking the end of underground coal extraction in the Durham and Northumberland Coalfields.

Table 1: Summary of the mining history of the UK and Durham and Northumberland Coalfields. References; 1) Bell (1986), 2) Bruyn & Bell (1999), 3) Smails (1935), 4) Healy & Head (1984), 8) Fielding (1982), 9) Dearman et al. (2000), 10) Page (1907), 11) Smailes (1938), 12) Nef (1965), 13) Galloway (1898).

3 Methods

High-resolution sedimentary logs of 9 vertical sections, spaced every metre, were taken along the workings exposed near Whitley Bay (see Figure 3). Lithological boundaries, both structural and depositional, were defined as either based on a distinct change in grain-size, or matrix type. The relationship between sedimentary facies within the workings can be split into two areas, pillars and stalls, depending on whether unworked coal is present or absent respectively in the logged section (Fig. 3). A sedimentary log through the unworked High Main Seam at the base of Hartley Steps (British National Grid: NZ 34469 75668) was taken as the comparative baseline for the collapse lithologies. Facies were defined based on distinct changes in texture, grain size, stacking relationships and sedimentary structures. Collapse breccias were described using the terminology of Woodcock & Mort (2008), who define chaotic, mosaic and crackle breccias based on clast size and ratio of clast to matrix. The clast type, orientation (taken as the dip of preserved bedding) and aspect ratio were recorded, along with the matrix composition. Muds in the sequence, which were not lithified, were described using the BS5930 (2015) standard for clay-rich soils.

Photographs (320 images) were taken of the outcrop to create a high resolution, orthorectified, photomontage (Fig. 3). Using the sedimentological information and location of logged sections, key boundaries were mapped out and stacking relationships investigated. Within the collapse breccia, a number of sub-divisions could be defined with subtle changes in clast orientation observed (e.g. 45 and 82 cm in Log 1). These areas were used to help constrain the phases of collapse recorded in the sequence.

4 Results

4.1 General description

Eight facies were identified through detailed field observations and sedimentary logging (Table 2). Two stalls are observed at Whitley Bay, which make up 69% of the outcrop. Both lithologies that overlie the High Main Seam in the central pillar and edge of the northern pillar display similar facies associations (Fig. 3).

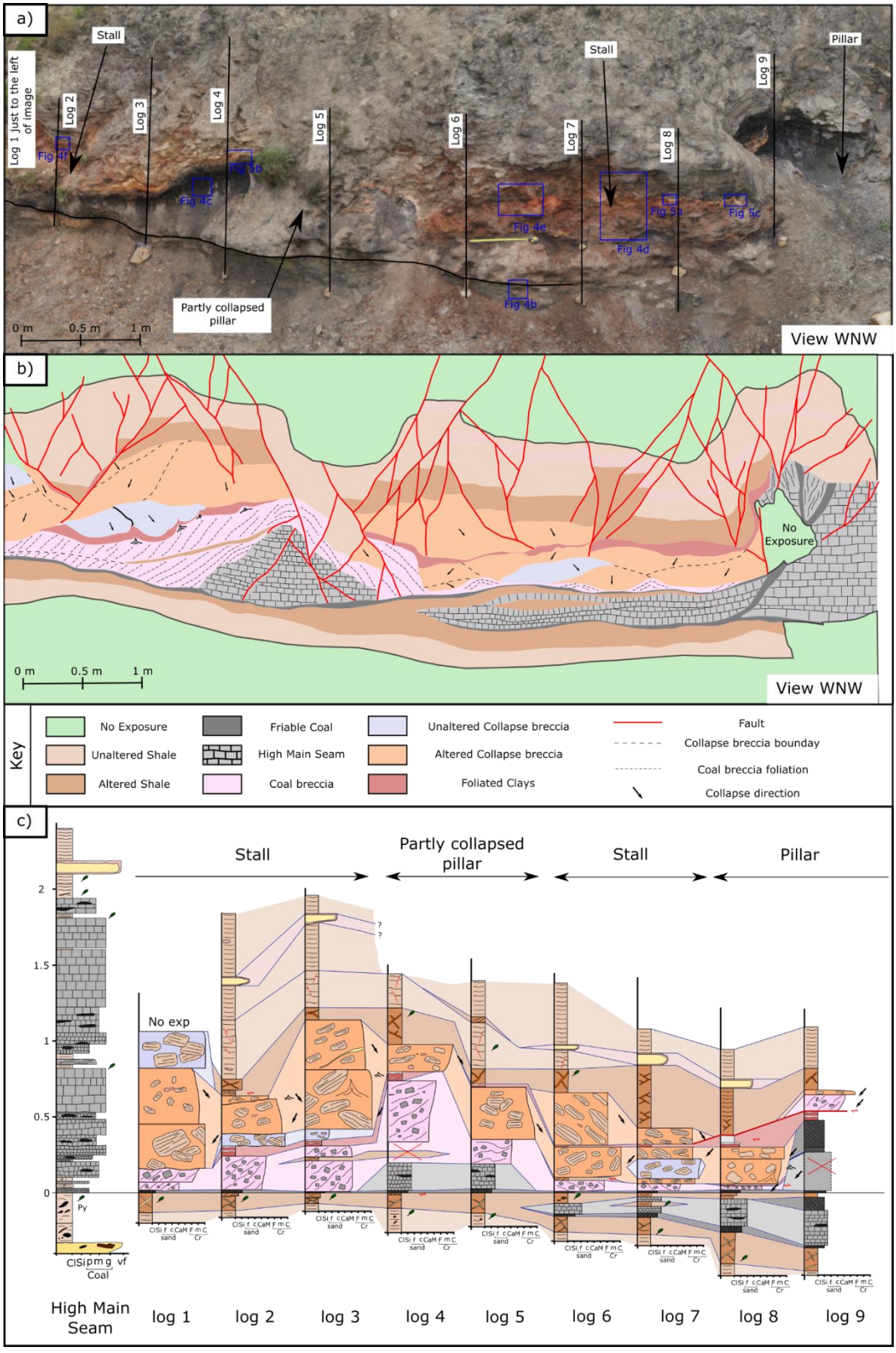

Figure 3: Workings of the High Main Seam near Whitley Bay: a) photomontage of the workings with the location of logs marked; b) section view and interpretation of mine wastes (collapse lithologies); and c) sedimentary logs through the undeformed High Main Seam at the base of Hartley Steps and through the workings at the locations marked in (a). For individual log descriptions please see Supplementary 1.

Facies	*Description*	*Depositional processes*
High Main Seam (HMS) Undeformed thickness = 2.01 m. Fig 4a	Interbedded unit containing 16 coal beds (2 to 43 cm thick) and 7 organic rich shale partings (1 to 4 cm thick). Euhedral pyrite crystals (<0.2 mm) occasionally visible along bedding planes. Locally Jarosite is developed along the cleat network, particularly towards the base of the High Main Seam.	The deposition of peat in a swampy, anoxic environment which was sporadically interrupted by clastic deposition in a delta plain environment[1].
Unaltered Shale (US) Beds 0.2 to 1 cm thick Fig 4b	A mudstone to silty-mudstone, which can be either organic rich or organic poor. Coalified plant fossils and euhedral pyrite (<0.2 mm, <5%) are often found along bedding surfaces, particularly below the HMS.	Low energy deposition in a variably oxic environment, related to the flooding of peat swamps[1,2].
Altered Shale (AS) Beds 0.2 to 0.8 cm Figs 4a & b	Found above and below the workings of the HMS in undeformed and worked sections. Similar to US, however, weathers more readily and contains shallowly dipping alteration planes (yellow below & brick orange above).	The development of acid mine water following mining operation causes the degradation of clay minerals and movement of the sulfur from the pyrite within the seam[3].
Friable Coal (FC) <15 cm thick. Figure 4b & d	FC may be observed along the base, and within the workings, as well as along the edge of the right-hand pillar (Figure 3). FC is black, dominated by organic material (> 95%) and characterised by a very tight fracture network which cause the lithology to erode as a black powder. Fractures either occur perpendicular to layering, or at an angle forming a well-developed foliation.	Can either be formed by working related deformation of thin channel coals and stringers of the HMS or the development of tectonically deformed coals[4] along the edge of pillars during the collapse of workings.
Coal Breccia (CB) Thickness 2 to 55 cm Figure 4c	CB occurs along the base of the workings, and varies in thickness considerably. CB is a chaotic to mosaic breccia[5] consisting of angular clasts of coal (>90%) and highly altered shale. Coal clasts (median 60 mm^2) are bounded by bedding planes or cleats. Shale clasts are often altered to a red-orange, silt to clay grade dust. The matrix is dominated (<95%) by silt grade organic fragments with the remaining 5% consisting of quartz and occasional <0.5 mm pyrite crystals.	May be formed either a) through the spalling of the pillars, whereby talus-like deposits occur as pillars corrode through time[6], b) through the down-dip flow of coal during flooding events being deposited in the lee side of pillar in a similar manner to sediment lags behind bridge abutments[7], or c) a product of waste being discarded behind miners during coal extraction that built up against pillars.
Collapse Breccia (CoB) Thickness 20 to 90 cm Figure 4d & e	The dominant lithology in the collapsed stalls CoB is found as altered or unaltered pods of clast dominated (85 to 90%) crackle breccia[5]. Clasts, are dominated by shale clasts (90 %), with clasts of ironstone, coal and bleach-white sandstone or seat earth also present. Clasts typically show high aspect ratios elongated parallel to bedding. The matrix is clay-rich containing brick-orange, silt grade clasts of altered shale and sand grains.	Rotation of clasts away from pillars as material collapses into the stalls[8]. Where the permeability of the workings is low, and mine water develops, clays in the collapse breccia degrade and develop the orange alteration colour.

Foliated Muds (FM) *Thickness 0.5 to 15 cm* *Figure 4f & 5*	FM consists of mm to cm scale foliated, unlithified muds which alternate between brick-red and off-white in coloration. Foliations typically stack from brick-red to white, with the top of the white foliations marking distinct depositional phases. Between 7 and 13 cycles can be identified, filling from the deepest point and occasionally showing soft-sediment deformation.	Cyclical flooding and evaporation of salt-rich fluids and mine water, causing a stacked sequence above the pre-existing CoB. The red foliations are likely caused by acid mine water reactions (see discussion for further details) forming ochre deposits. Slumps develop either due to rapid deposition on the CoB top topography, or due to the further collapse along the workings.

123 **Table 2: Facies description and interpretation of depositional environment. Here, 'thickness' refers to the vertical thickness of a bed,**
124 **pod, or lithology within the studied section. References: 1) Fielding (1984b); 2) Fielding (1982); 3) Younger et al. (2002); 4) Godyń**
125 **(2016); 5) after Woodcock & Mort (2008); 6) Martin & Maybee (2000); 7) Koken & Constantinescu (2008); 8) Lokhande et al. (2005).**

4.2 Stalls

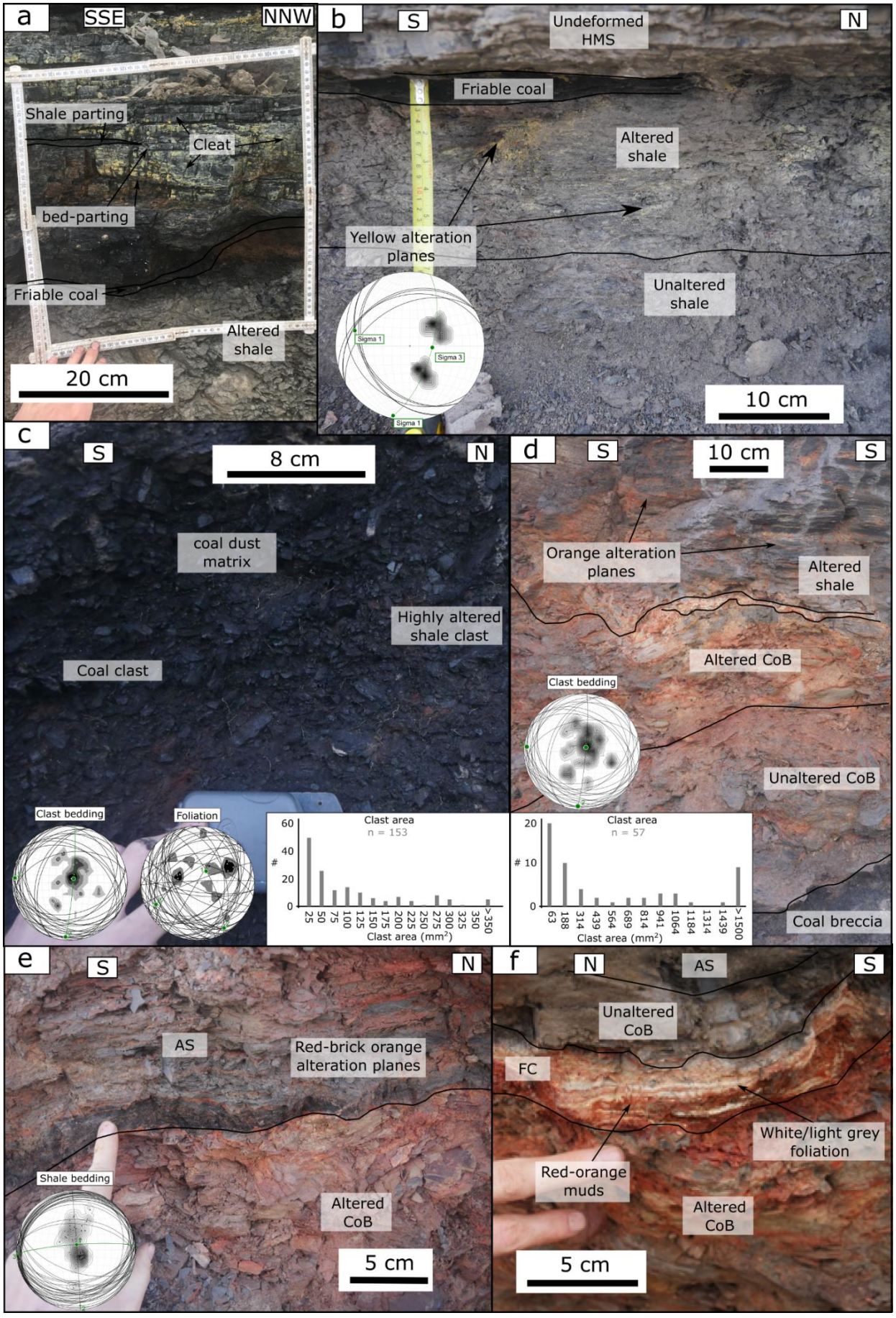
a
SSE
NNW
Shale parting
Cleat
bed-parting
Friable coal
Altered shale
20 cm
b
S
Undeformed HMS
N
Friable coal
Altered shale
Yellow alteration planes
Unaltered shale
Sigma 1
Sigma 3
Sigma 1
10 cm
c
S
8 cm
N
coal dust matrix
Highly altered shale clast
Coal clast
Clast bedding
Foliation
Clast area
n = 153
# 60 40 20 0
25 50 75 100 125 150 175 200 225 250 275 300 325 350 >350
Clast area (mm²)
d
S
10 cm
S
Orange alteration planes
Altered shale
Altered CoB
Clast bedding
Unaltered CoB
Clast area
n = 57
# 20 10 0
63 188 314 439 564 689 814 941 1064 1184 1314 1439 >1500
Clast area (mm²)
Coal breccia
e
S
N
AS
Red-brick orange alteration planes
Shale bedding
Altered CoB
5 cm
f
N
AS
S
Unaltered CoB
FC
White/light grey foliation
Red-orange muds
Altered CoB
5 cm

Figure 4: Facies photographs and associated clast and kinematic data. The location of the photographs for (b) to (f) is indicated on Figure 3. The photograph for (a) is taken at the base of Hartley Steps [British National Grid: NZ 34469 75668]. (a) undeformed High Main Seam with Jarosite developed along the cleats of the lowermost beds. (b) The succession underlying the High Main Seam, with the orientation of the yellow alteration planes shown in the inset stereographic projection. (c) Close up photograph of the coal breccia built up on the southern side of the central pillar. Inset stereographic projection display the orientation of clast bedding and the foliation picked out by fines. The inset histogram displays the equivalent circular area of all clasts measured in the field (n = 152). (d) The succession overlying the coal breccia. CoB = collapse breccia. The inset stereographic projection displays the orientation of bedding in the CoB clasts, with in inset histogram displaying the equivalent circular area of the clasts. (e) The contact between altered shale (AS) and Altered collapse breccia (CoB) at the top of the collapse lithologies. The insert stereographic projection displays the bedding of the altered and unaltered shale overlying the collapsed workings. (f) The development of the foliated muds above altered collapse breccia (CoB) towards the south of the outcrop.

The thickness of the collapsed stalls, defined as the distance between the laterally continuous friable coal at the base of the workings, and the fractured unaltered shale at the top, ranges from 52 cm in log 7 to 114 cm in log 3 with the collapse facies thicknesses and associations varying along the outcrop (Fig. 3c). The relationships of unaltered shale, altered shale and friable coal are the same as the undeformed section; however, the thickness of altered shale is greater beneath stalls. Coal breccia can be observed on-lapping onto the partially collapsed pillar (Fig. 3b), with the maximum thickness (c 40 cm) and larger clast sizes (median = 144 mm^2) found closest to the boundary of the pillar (Fig 4c). Coal breccia does not show clear grading; however, a weak foliation is picked out by fines that dip and away from the pillar (Fig. 3c, 4c). Towards the south of the outcrop coal breccia occurs as a discontinuous layer, with the foliation suggesting that soft-sediment deformation caused by later collapses caused the thinning and thickening of the unit.

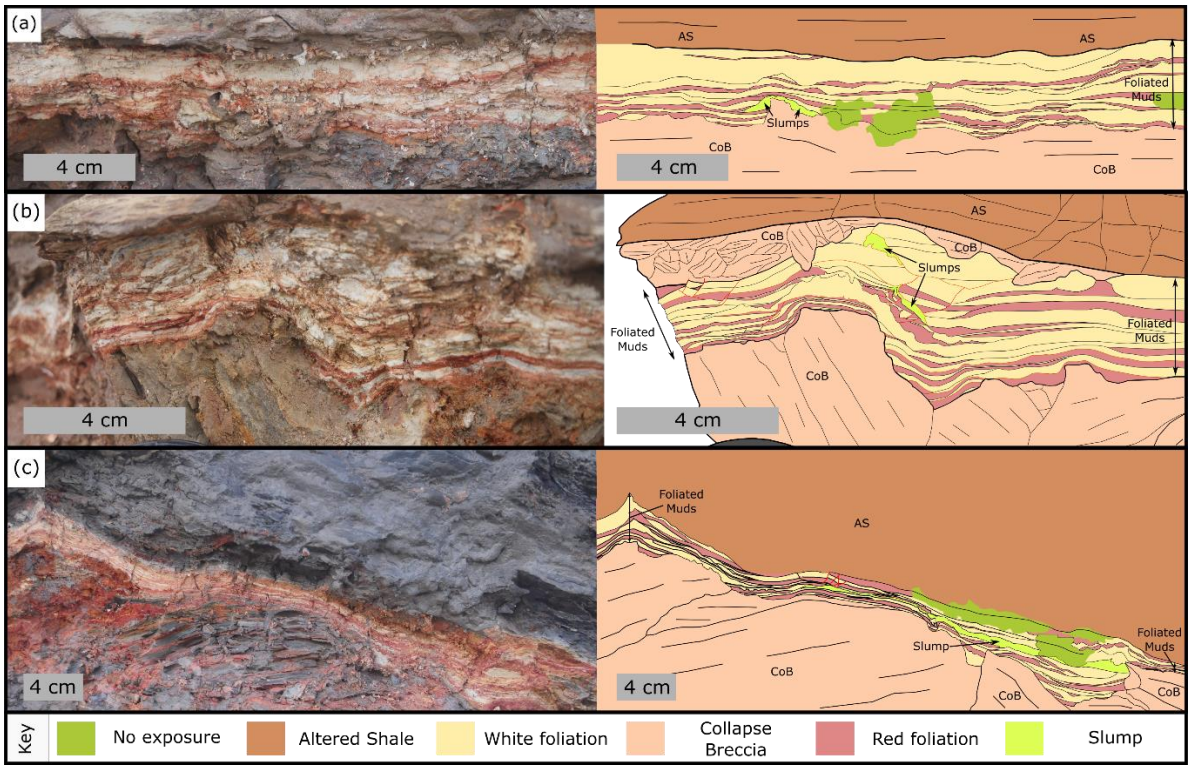

Figure 5: FC stacking patterns. The location of the detailed photographs are indicated on Figure 3. Please see text for a description of key features.

Foliated muds typically dip towards the SW and are observed in both stalls, overlying coal breccia in the south stall and either coal breccia or collapse breccia in the north stall. Complex stacking patterns and sedimentary structures are observed in the foliated muds, which are controlled by the underlying topography (Fig. 5). The alternating red- and white- layers are cyclical in nature, with the number of cycles varying from 7 to 13. At the base of foliated muds, the foliation can be seen to on-lap onto angular clasts of collapse breccia, with the thickest deposits occurring in gaps between clasts of collapse breccia (Fig. 3). This shows that the collapse occurred after mining and was followed by the deposition of the foliated muds, which filled the topography on the top of the collapse breccia. Stacking patterns in Fig. 5a suggest that rotation of this topography occurred throughout the deposition of the muds, leading to changes in depocenters probably caused by further collapse of workings disrupting the collapse breccia.

The bottom of the foliated muds is generally undisturbed, however, in the mid- to upper- sections of the deposit slumps, minor faulting and soft sediment deformation can be observed. Slumps occur where a paleoslope occurs either within the foliated muds or from the top of the collapse breccia. For example, in Fig. 5c a laterally extensive slump deposit is observed, with normal faults developed at its head, and compressional features at its foot. This can be observed along the shallowly dipping (c. 8° to 10°) upper surface of the collapse breccia. In Fig. 5b, the top of the foliated muds has been deformed by a later collapse, which caused the soft-sediment deformation of a thick white layer, and small-scale faults and foliation rotation to develop.

Foliated muds may either be overlain by further collapses (collapse breccia), which often caused soft-sediment deformation of the pre-existing units, or, to the far north of the outcrop, by altered shale. Altered shale makes up the top of the collapse lithologies and is brought down onto underlying lithologies by a series of fault strands that led to the closing of open space (Fig. 5b) and the extrusion of foliated muds along the edge of the pillar (Fig. 6a).

4.3 Pillars

Two pillars are observed, which make up 31% of the outcrop width: one to the north and another near the centre of the studied section. In the northern pillar, the top 0.45 m of the undeformed High Main Seam succession is observed and the base is visible in the foreshore up-dip of the studied section; suggesting that the full thickness

of the seam (c. 2 m) is present at this location. The base of the High Main Seam exposed in the centre of the outcrop (logs 4 and 5) closely matches the lower part of the log of the undeformed sequence (Fig. 3c). However, above the undeformed coal in log 4 and 5, 14 to >40 cms of coal breccia are observed. This displays a subtle foliation, which dips away from the pillar and contains semi-randomly orientated clasts (Fig. 4c). Above the coal breccia, the central pillar shows facies associations more similar to that observed in the stalls (see above). The unaltered shale at both locations display low-amplitude folding (Fig. 4e), with material subsiding from above the pillars into stalls (See Fig. 3).

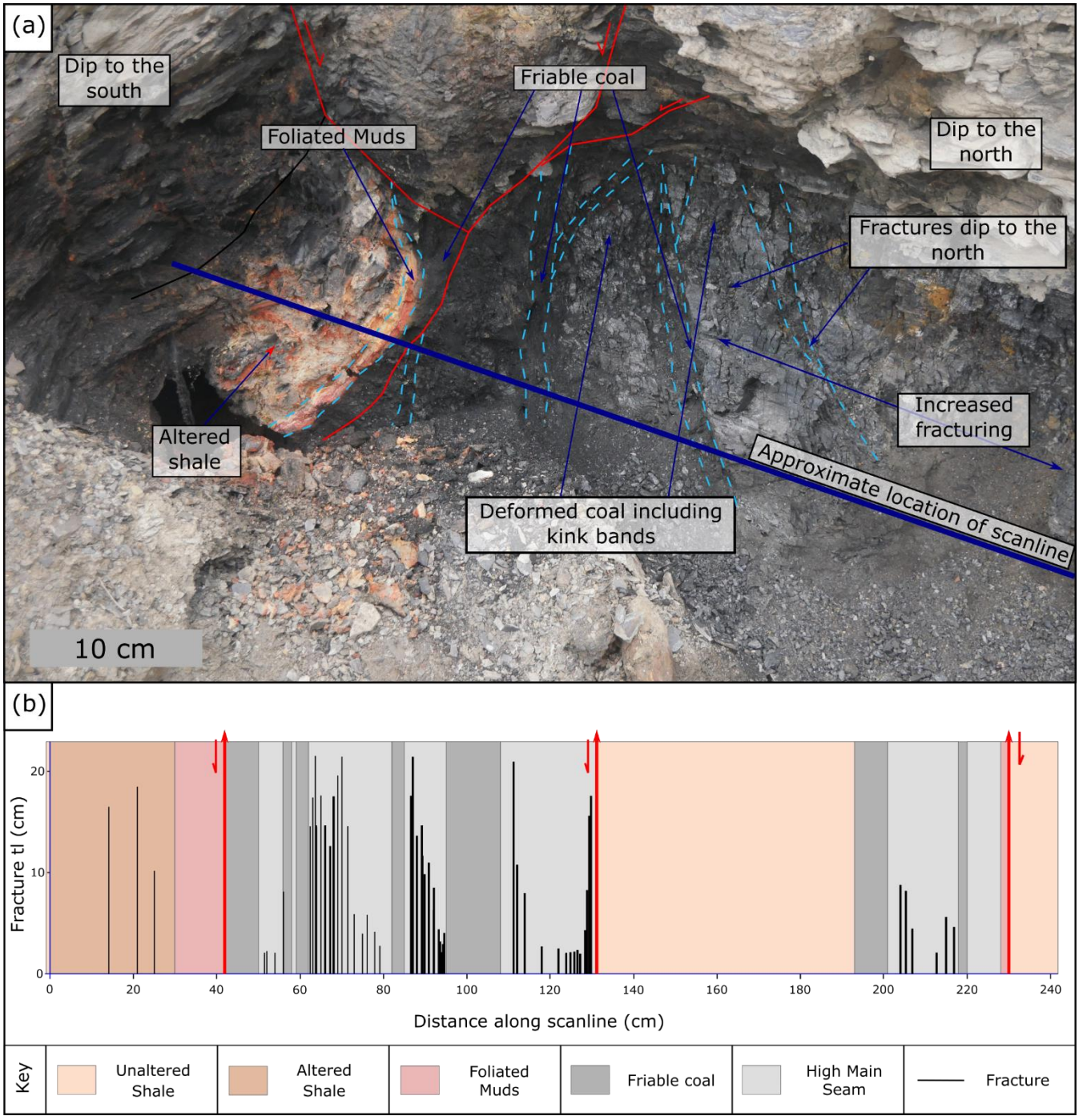

Figure 6: View looking W and down slightly at a slightly caved certical section that includes the northern Pillar: a) annotated field photograph displaying key structural elements of the edge of the northern pillar; b) scanline orientated orthogonal and passing through the edge of the pillar displaying the trace length of fractures. The location of the scanline is highlighted in a.

In both pillars the High Main Seam displays increased fracturing compared to the undeformed section, along with local development of friable coal (Fig. 6). The scanline taken through the northern pillar (Fig. 6b), highlights that within 5 cm of the friable coal the trace length and intensity of fractures increases. Fractures often form parallel to, and utilised, the pre-existing cleat network. Locally, particularly between strands of friable coal, bedding, cleats, and fractures are rotated (Fig. 6a). This suggests that fracturing occurred prior to the block rotation of the

coal, and that only later deformation (e.g. development of kink-bands) occurred during the development of friable coal.

Bedding orientation below the High Main Seam is similar to the seam itself (040°/10° W), however, bedding above the seam maintains thickness and dips to the north and south with a mean fold axis of 105°/80° N (Insert Fig. 4a). Folding is subtle above stalls, however, above pillars it is clearly visible. At this location the folding and rotation of bedding along antithetic faults occurs such that two low amplitude open anticlines and three synclines with wavelengths of 0.5 m to 2 m are observed. This suggests folding is due to the sagging of the overburden following roof collapse.

4.4 Comparison between the sedimentology of mine and cave collapse.

A good analogue for the lithologies and processes described in this study is the collapse and sedimentation of modern and paleo-cave systems (e.g. Labourdette et al., 2007; Loucks, 2007, 1999; McMechan et al., 2002). This provides a useful conceptual framework to understand the observed lithologies and stacking patterns that outcrop near Whitley Bay. Loucks *et al.* (2004) identified 5 distinct paleo-cave facies from core and outcrop data showing clear parallels to the facies observed near Whitley Bay (Table 3). The key differences in the depositional systems include: the thickness and lateral extent of the facies; properties of the zone of damage; initial lithological properties; and finally that the collapsed mine workings leave a low permeability, clay-rich layer and not a highly permeable coarse chaotic collapse breccia (Loucks et al., 2004).

Cave collapse facies Louchs et al. (2004)	Equivalent mine collapse facies identified in this study
Continuous Strata Facies: Competent, coherent bedded carbonates, with only local evidence of deformation.	Interbedded siliciclastic lithologies with high clay content in the succession.
Discontinuous Strata Facies: Characterised by localised folding and faulting, with some local brecciation. Bedding is generally continuous along strikes. The unit is highly fractured and has local development of mosaic breccia.	Localised faulting and the rotation of bedding is observed; however, bedding can still be observed.
Highly Disturbed Strata Facies: Highly deformed, discontinuous bedded strata with considerable amounts of crackle and mosaic brecciation. Small scale fault and folding common and interbeds of clastic material mark where individual collapse events are recorded. Interacting deformation patterns only occurs where two sections of caves are in close proximity.	Immediately above the worked seams deformation commonly interacts with deformation patterns from nearby stalls (Stage 3,.
Coarse-Clast chaotic breccia facies: Very poorly sorted, matric to clast-supported granule-to boulder-sized chaotic breccia. Finer interbeds common, interpreted as sediment transport into the cave (Loucks, 1999). Overall volume of collapsed lithology increase by c. 40% (Labourdette et al., 2007). Where available rock is less than 2.5 times the volume a collapse sinkhole develops (e.g. Mylroie et al., 1995).	Similar to the collapse breccia, however, due to the shale roof of the High Main Seam, lower expansion of the breccia occurs during collapse, permeability will be low and only a small space is available to be filled with fines. The collapse of shallow workings can lead to sink hole development (Garrard and Taylor, 1988; Poulsen and Shen, 2013).
Fine Chaotic Breccia: Poorly to well sorted, matrix to clast-supported, granule- to cobble-sized chaotic breccia. Sediment fill commonly observed, but limited to small grain size. Sediment fill deposited by transport from within or outside the cave (Loucks, 1999).	Coal breccia develops from material left from mining operations and the spalling of pillars (Martin and Maybee, 2000). This then gets transported along the coal seam.
Finer Grained Sediment Facies: Consist of silt- to granular-size sediment, dominated by detrital carbonate. Siliciclastic clay may reach 4%, but generally accounts for less than 1%. Sediment is interpreted as being transported in an open chamber by traction, mass-flow and suspension mechanisms.	Foliated muds deposited from the mixing of mine-waters and deep hyper-saline brines leading to the sedimentation of thin muds from evaporation, suspension and mass transport mechanisms.

Table 3: Comparison between cave collapse lithologies and those observed in this study.

5 Discussion

5.1. Processes involved in the formation of collapsed pillar and stall workings

We investigated the processes which occur during the collapse of abandoned pillar and stall mine workings. For the first time a conceptual evolutionary model for the temporal evolution of the internal structure is proposed based on detailed sedimentological and structural evidence. This has allowed the processes which occur during collapse to be proposed. Five distinct phases are identified, as outlined below and summarised in Fig. 7.

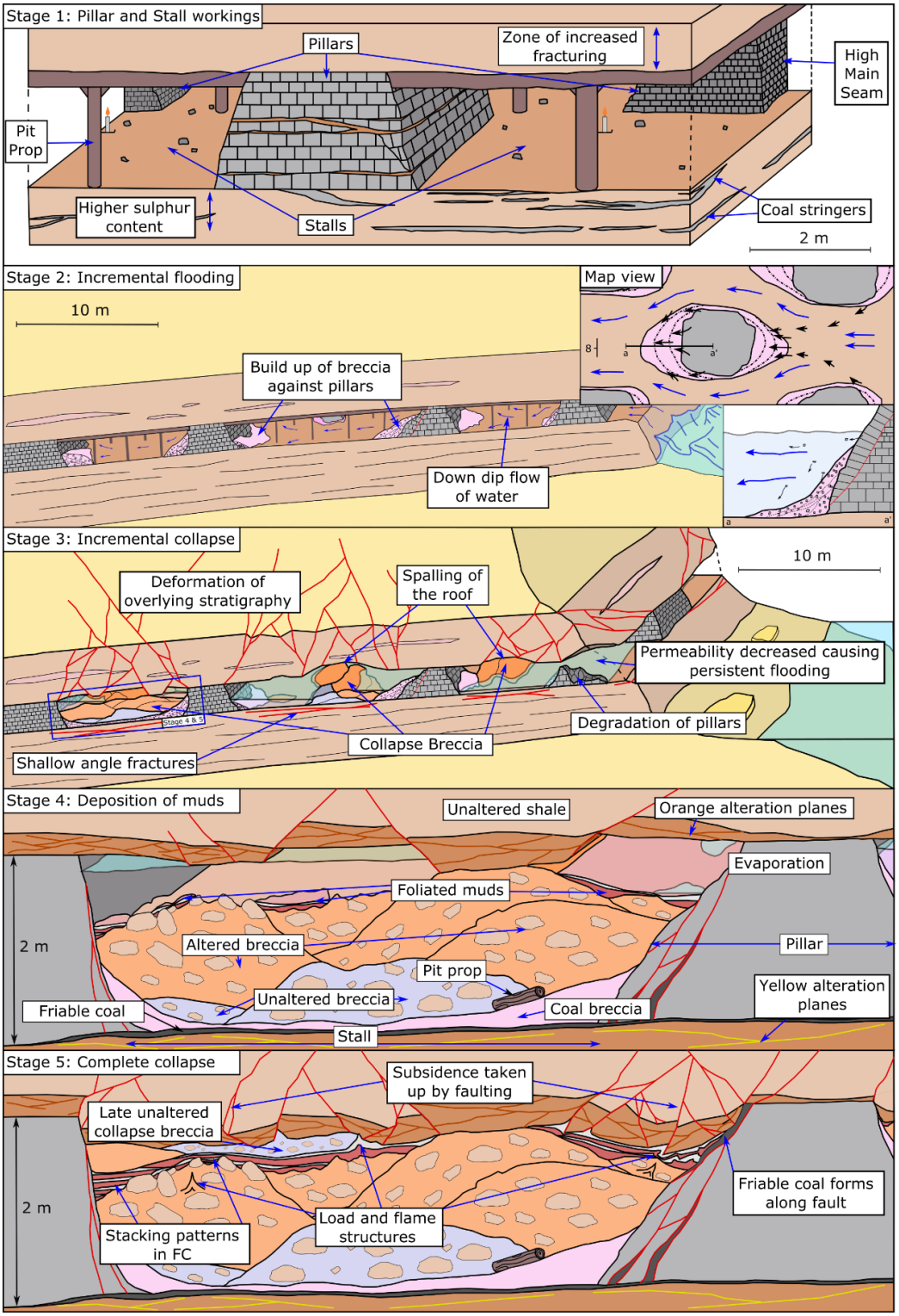

Figure 7: Conceptual evolutionary model of the collapse of pillar and stall mine workings based on Whitley Bay, Northumberland. See text for description of each stage.

Stage 1 & 2: Extraction of coal and build-up of CB:

The High Main Seam was worked using pillar and stall mining methods, sometime between 1550 and 1710 AD (see Table 1). The shallow depth of the seam at this location suggests that access was most likely from an inclined adit driven upwards from the beach (a sea drift). The proximity to the coast, current

seam level, probable adit height, and early date of the workings (pre-pumping technology) supports the interpretation that the outcrop near Whitley Bay was worked above the water table. Lying above the water table, workings would drain under gravity via the adit, so flooding likely only occurred following periods of heavy rain and/or winter storms. During the extraction of coal, small fragments of low-value coal and coal dust would be left behind. These would have been transported down-stream (towards the SW) during flood events and deposited against pillars, leading to the development of the coal breccia. The on-lapping of coal breccia onto the degraded pillar (Fig. 3b), the orientation of the faint foliation (Fig. 4c), and clast-bedding orientation (Fig. 4c) matches the deposition pattern that would be expected in a shallow channel flowing around an obstacle (e.g. scouring around groynes (Koken and Constantinescu, 2008)). Separation of coal by density to form a coal "lag" is typical in streams and beaches. Following the end of mining operations pillars began to spall and collapse (Salmi et al., 2019). Larger clasts of (higher value) coal would then added to the breccia from pillar spalling and collapse (**Stage 2**). Another possible interpreation is that the coal breccia represents an anthropogenic deposit caused by miners discarding waste material behind them during coal extraction. However, we feel this is less likely due to the grading and stacking patterns observed in outctop (Fig. 4c).

Stage 3: Incremental collapse and steady reduction in permeability:

As time passed, we suggest that episodic flooding degraded pillars and pit-props and the roof of the workings began to sag and spall (e.g. Bruyn & Bell 1999). Onlapping relationships suggest the collapse near Whitley Bay occurred through a total of 19 events (Fig. 3b). In agreement with the work of Helm *et al.* (2013), we suggest collapse initiates near the centre of stalls, as evidenced though stacking patterns and sedimentary structures (e.g. slumps) observed across the outcrop, and that this was followed by several small collapses propagating towards the pillars. Initially collapses likely did little to reduce the overall permeability of the workings, and episodic flood waters would flow around the collapsed sections. As the percentage of collapsed material increased, clays sourced from shales would clog pore-space between clasts. The breccia, which was poorly sorted and already had a low permeability, would have become saturated.

Mine water is typically acidic (Younger, 2004, 1995), a product of both 'vestigial acidity' caused by the previous oxidation of pyrite, and 'juvenile acidity' caused by the products of seasonal pyrite oxidation above a fluctuating water table (Younger, 1998). A complex cycle of chemical reactions takes place as pyrite oxidises (See Stumm and Morgan, (1981) for full description). However, the simplified net products can be described through Equation 1, with the overall sequence being acid-producing (Equation 2) (Banks et al., 1997):

$$2FeS_2 + 2H_2O + 7O_2 = 2Fe^{2+} + 4{SO_4}^{2-} + 4H^+_{(aq)} \quad \text{(Equation 1)}$$

$$Pyrite + water + oxygen = ferrous\ iron + sulphate + acid$$

$$4FeS_2 + 14H_2O + 15O_2 = 4Fe(OH)_3 + 8{SO_4}^{2-} + 16H^+_{(aq)} \quad \text{(Equation 2)}$$

While little pyrite oxidation will take place below the water level, oxidation will be abundant in the unsaturated zone with the reaction products mobilised as ground water rises (Younger, 1993; Younger and Sherwood, 1993). The high acidity and oxidising environment represents the ideal situation for the development of ochre (Younger et al., 2002). Ferrous iron released by the oxidation of pyrite will remain in solution while acidity is particularly high (pH < 2.5) or where oxygen levels are reduced (e.g. fully saturated workings) (Banks et al., 1997; Younger et al., 2002). However, when the ferrous iron is exposed to the atmosphere partial oxidation will occur leading to the precipitation of ion oxyhydroxide (ochre) (equation 3 and 4) (Banks et al., 1997).

$$4Fe^{2+} + O_2 + 4H^+ \rightarrow 4Fe^{3+} + H_2O \quad \text{(Equation 3)}$$

$$Fe^{3+} + 3H_2O = FeOOH + H_2O + 3H^+ = Fe(OH)_3 + 3H^+ \quad \text{(Equation 4)}$$

The pyrite within the saturated collapse breccia would have been oxidised to form weakly acidic mine waters (Turner and Richardson, 2004; Younger, 1995, 1994), which altered clays in the matrix and clasts of the collapse breccia and mobilised iron from the siderite ironstone nodules/beds. This oxidation and leaching caused the red-orange coloration and bleaching respectively. The presence of breccia pods that do not show alteration suggests that some earlier and later collapses were not exposed to oxygenated groundwaters to the same degree, possibly due to being fully saturated with anoxic groundwaters or hydrogeologically isolated.

Stage 4: Formation of the foliated muds.

In the Durham and Northumberland coalfields, hypersaline barite rich brines (Younger, 1995), led locally to the development of Baryte ($BaSO_4$) and Witherite ($BaCO_3$) veins within the Westphalian Coal Measures (Dunham, 1983), which in places have been mined (Dunham, 1948). The Eccles Colliery, located 5.5 km west of the field site (British National Grid = NZ 304 695), primarily worked both the Main and High Main Seams and had problems with barium-rich groundwater (Gray and Judd, 2003). This required the installation of a Blanc-fixé plant that produced around 3000 tons of $BaSO_4$ per year (Palumbo-Roe and Colman, 2010). Alternation of Ba-rich brines with acidic minewaters could have led to the alternate deposition of baryte and ochre in the abandoned mineworkings, mimicking the mixing reaction used for the industrial process. Witherite is almost exclusively produced through the precipitation of barium sulphide solutions with either carbon dioxide (equations 5 & 6) or soda (Kresse et al., 2007). CO_2, locally termed blackdamp, is abundant within coalmine workings and the evidence from Whitley Bay suggests the workings were periodically flooded, providing H_2O into the system (Stage 1-3). Therefore, given the likely presence in the mineworkings of sulphate-reducing bacteria, conditions may have been present for the precipitation of witherite from upwelling barium rich hypersaline fluids.

$$2BaS + CO_2 + H_2O = BaCO_3 + Ba(HS)_2 \quad \text{(Equation 5)}$$

$$Ba(HS)_2 + CO_2 + H_2O = BaCO_3 + 2H_2S \quad \text{(Equation 6)}$$

Due to the presence of both altered and unaltered collapse breccia (Figure 3b), we suggest that the water table, and hence the composition of groundwater, varied through time. As groundwater levels rise due to meteoric water inputs, the products of pyrite oxidation will dissolve and the acidity of the groundwater will increase (as discussed in Stage 3). This will cause the proportion of acidic mine water relative to brines to increase and promote the breakdown of clays within the shales (Younger et al., 2002), which become entrained into the hypersaline fluid and carried in suspension. When the meteoric input and flow rate decreased, lower water levels would lead to the deposition of the red-mud layer. At times when pyrite oxidation was lower, the brine component of groundwater would have dominated and less clays would be held in suspension. This would lead to the deposition/precipitation of salty muds (possibly with light-

coloured baryte or witherite precipitates) in place of the red muds. The cyclic nature of the deposit (Figure 5) could thus be caused by annual groundwater fluctuations and if this is the case the foliated muds represent deposition over a 7 to 13 year period.

Given that the clays are deposited in thin layers preserved as the red foliation, this suggests periods of very little flow to enable clays to settle from suspension. The orange-red colour and silt-grade grains are similar to the altered shale clasts in the coal breccia, and likely represent clays sourced from shales altered by acid mine waters (c.f. Younger 1995). The top of each cycle is white to off white, clay-rich layers with a distinct salt-and-vinegar taste interpreted as precipitates from a hyper-saline fluid. The deposits would first have built up as small pods in topographic lows on top of collapse breccias, suggesting that the hyper-saline fluid formed puddles on the breccia, and that deposition through evaporation occurred prior to the next pulse. This type of deposit is commonly seen where brines periodically flood areas of topography (in this case the mine floor), essentially acting as a mini-basin which is infilled during reflux (Warren, 2016).

Slump-deposits and soft sediment deformation within foliated muds is seen either a) where the dip of the paleo-topography is high (>8°), or b) in the vicinity of later collapse breccia pods (Fig. 5). Slump deposits may either have been caused by the rapid build-up of sediment on a slope (Moore, 1961), or following ground motions, for example earthquakes (Keefer, 1984) or local collapse. Both processes could have been active in the workings, with pulses of saline brines and/or flooding during winter storms causing rapid deposition of muds and evaporites and ground motion caused by roof collapse. The slump deposits in both Fig. 5a and b show no disruption of overlying layers, and have upright folds at the toe following an ‘open-toe’ deposition style with units above on-lapping onto the deposit (c.f. Alsop *et al.* 2016). In contrast the deposit in Fig. 5c has a longer run out, is thicker and overlying cycles are deformed through normal faulting at the head and compressional features at the toe. We suggest the slumps in Fig. 5 a and b formed due to rapid sedimentation on the paleo-topography present on the top of the collapse breccia, possibly triggered by minor collapses. Fig. 5c, however, was deposited following a roof collapse which caused a slump to develop, utilising a shallowly dipping clay layer as a decollement, similar to large scale processes caused by earthquakes (Alsop et al., 2016). Collapse related slumps are found at different stratigraphic layers within the foliated muds, suggesting that the workings collapsed over several years.

Stage 5: Final collapse of stall:

Eventually pillars degraded to the point where they could no longer support the overlying stratigraphy and the roof collapsed. The collapse and subsidence of overlying units has been accommodated through normal faults which dip away from the zone of collapse. This caused triangular zones of deformation, with subsidiary faults coming off the main strands (Fig. 3). The minor faulting pattern was controlled by the topography of the pre-existing collapse lithologies. For example, to the north of the partially collapsed pillar material was brought down by several small offset fault strands which bound 'lenses' (c.f. Gabrielsen *et al.* (2016)) of undeformed shale and ironstone.

The orange alteration of the collapse lithologies near Whitley Bay (Fig. 4) suggests that they were at least partially saturated at the time of collapse, with soft sediment deformation observed in collapse breccias, foliated muds, and coal breccias (Figs. 3b, 5). While Stage 5 occurred following the deposition of foliated muds to the north of the outcrop, in the rest of the outcrop Stage 4 is followed by a return of Stage 3 and the deposition of collapse breccia pods (Fig. 3). Where collapse breccia is not found, foliated mud is thickest with the greatest number of cycles observed (13 as compared to 7 to 8 to the south). This suggests that the void near pillars was open to flow far longer that the rest of the workings.

5.2. Relevance to deeper pillar and stall workings

When considering the applicability of the processes of collapse interpreted at Whitley Bay to mine workings at a depth that could represent a geothermal prospect several mine-specific factors need to be considered as outlined below:

1. ***Pillar geometries and distribution***: Pillar properties (e.g. geometry, distribution, and width to height ratio) strongly effects how prone a section of a mine is to collapse (Garrard and Taylor, 1988; Taylor and Fowell, 2007). The geometry and distribution of pillars varied between coal fields (Figure 1) and within individual collieries in response to geological conditions (e.g. faulting) (Bruyn and Bell, 1999). Due to the economic importance of coal and governmental regulations, detailed plans of mine layouts at the time of extraction are common place, with the UK making it a legal requirement in 1872 (Bell, 1986). The recorded mine layout of seam worked by pillar and stall methods may however become altered by pillar

spalling (Salamon et al., 1998), changes in local stress (e.g. collapse of nearby pillars (Zhou et al., 2019)), and environmental factors (e.g. strength reduction through wetting) (Fang and Harrison, 2002; Salamon et al., 1998; Zhao et al., 2016). Additionally, the spalling of roof material can increase the effective seam height (Salamon et al., 1998). These factors could lead to a highly heterogeneous pattern of collapse (e.g. (Poulsen and Shen, 2013; Zhou et al., 2019)).

2. ***How widespread was the use of pit props?:*** The use of timber supports in mining was described by Agricola in De Re Metallica in 1556 (e.g. p 124-5). However, the use of pit-props was an innovation in Tyneside around 1800 which allowed for extraction of a greater proportion of coal (> c.40%) and were used for temporary support where the span between pillars is effectively too large for the pillars alone to support the roof. Pit-props were widespread in the Northumberland and Durham coalfields, with wood fragments observed in borehole logs intersecting early workings of seams overlain by shale roofs (e.g. Workings of the Low Main Seam, Eccles Colliery [NZ 428080 574320])***.*** However, the use of pit-props varied throughout the UK (e.g. Daunton, 1981) and globally, depending on requirements due to differing roof lithologies and/or local extraction methods (e.g. Ayrshire short-wall, surface mining).
3. ***Multiple mining levels:*** In mature mining areas (e.g. Northumberland) it is common for seams at different levels to have been worked from the same colliery. For example, the Hartley Colliery located just inland from the studied section [NZ 301 771], worked the High Main and Yard seams primarily by pillar and stall methods, and the Five Quarter seam initially by pillar and stall methods, followed by later longwall mining. The undermining of pillar and stall workings affects the local stress regime in the mine, and will impact the location and extent of collapses (Zhu et al., 2018).
4. ***Pillar robbing:*** The removal ("goafing") or partial extraction of coal from pillars during the final stages of mining, termed 'robbing of pillars', was commonly practiced (Brady and Brown, 1985), and evidenced on mine abandonment plans of the High Main Seam at Seaton Delaval Colliery [NZ299763]. Pillar robbing on retreat reduces the effective strength of the pillars by increasing the span to height ratio, and can promote roof collapse (Poulsen and Shen, 2013; Salamon et al., 1998).
5. ***Stowage, loose or packed waste, and backfill:*** Across many coalfields (e.g. Ayrshire and Glasgow) it was common place for miners to 'backfill' mined out voids with waste material (e.g. sandstone, foul coal, and

seat-earth fragments) (e.g. Karfakis et al., 1996). The workings in this study are clearly not backfilled due to:

a. ***Differential compaction around shale fragments in the collapse breccia:*** In packed waste you would expect compaction to occur over a period of time and compaction potentially occurring orthogonal to bedding. You would also not expect to see the differentiation between siltstone and mudstone layers that are observed in the altered shale (Figure 3) and subtly in the collapse breccia (Figure 4d-f) in packed waste.

b. Presence of foliated muds and slump deposits: For foliated muds to develop (Figure 4 & 5), void space is required for a significant period of time, that is periodically disrupted causing the observed slump deposits (Figure 5). The use of backfill in sub-surface mining was a useful way of discarding waste without having to haul it to the surface and therefore areas of packed waste would have been densely filled from floor to roof.

c. Stacking patterns and facies associations across the studied section: In packed waste you would not expect to able to observe distinct facies relationships (Figure 3) and clast orientations (Figure 4) that are observed across the outcrop.

Clear differences in lithology and stacking patterns are expected between the section studied at Whitley Bay and a backfilled stall and therefore a similar sedimentological approach used in this study is required to classify packed waste.

6. ***Rising water levels:*** Following mining operations, post-mining ground water rebound causes mines to flood (Younger et al., 2002) leading to the degradation and strength reduction of pillars and transport of fine grained material in a similar manner to cave systems (Table 3). In exceptional cases (e.g. through a combination of faulting and collapse) it may even possible for workings to remain unsaturated for many years after other areas of the colliery have flooded.
7. ***Stratigraphic relationships****:* In typical coal-bearing sequences the overlying stratigraphy of different seams can be somewhat variable, with sandstone and shale roofs common (e.g. Fielding, 1984a,b). When collapse occurs, a vertically propagating fracture network will develop; however, the height of the fractured zone depends on the nature of the overburden (Garrard and Taylor, 1988; Taylor and Fowell,

2007), in particular the presence of any 'key strata' (e.g. competent sandstone beds also called 'Sandstone Posts') (Miao et al., 2011). In coal measures, a general 'rule of thumb' approach has been devised for the maximum extent of subsidence of 10 times the seam thickness (Garrard and Taylor, 1988; Poulsen and Shen, 2013; Taylor and Fowell, 2007);. Coal seams rarely only consist of coal, but instead contain several 'bands' or 'partings' of siliciclastic material (see the High Main Seam in Figure 3). The presence of partings effects the strength of pillars, and therefore likelihood of collapse and spalling (Kaiser and Cai, 2012; Liu et al., 2019). Additionally, where coal seams are underlain by clay rich lithologies the seam floor can rise up into stalls through clay swelling, which was known issue in the Durham and Northumberland Coal fields (Jenkins, 1958). Otherwise the material that overlies and makes up the seam will constitute the majority of the collapse fill, and therefore strongly impact the nature of the mine-waste. Fills consisting of a high sandstone content will likely contain gaps between clasts, along with a greater permeability within clasts, compared to a fill consisting of predominantly shale.

8. ***Presence of Faults:*** Miners typically aligned pillars such that they were elongated sub-parallel to faults and worked the coal until it was no-longer safe and/or economic to do so. Faults in coal measures tend to be structurally weak (Donnelly et al., 2008) and prone to reactivation causing a significant geotechnical risk to surface infrastructure (Bruyn and Bell, 1999; Donnelly, 2006).

The above factors raise uncertainties in understanding the lithologies present after stall collapse when these are intersected in boreholes inland. The Burradon House Borehole [NZ 427390 573130] intersected collapse lithologies from pillar and stall workings of the High Main Seam (113.69 m) worked in 1900. The base of the seam consist of 2.51 m of shale and fireclay (shale rich paleosoil), that is broken and fragmented with rusty weathering patterns (equivalent to Collapse Breccia). This is overlain by 0.74 m of mixed fragmented shale with rusty weathering and intact grey siltstone (equivalent to the Altered Shale). Finally, 1.17 m of shale with rusty weathering, and a shale with hematite stained ironstone nodules and plant material is recorded (equivalent to unaltered shale). The borehole, sunk prior reworking by longwall methods, also intersects workings of the Yard Seam (165 m). Unlike the High Main Seam, the Yard Seam (c. 1m thick) is overlain by a 5 to 8 m thick sandstone succession, and the borehole records 0.38 m of waste consisting of shale, broken fine-grained sandstone and suspected cavities.

Inland boreholes suggest lithologies described in this study are comparable to collapses of similar stratigraphic successions at depths that could act as a geothermal reservoir. Additionally, the level of detail possible using a sedimentological approach allowed collapse processes to be interpreted. We therefore suggest that a similar approach is undertaken at several near-surface sites, particular those with different roof lithologies and mining methods, to enable the full range of collapse facies and processes for pillar and stall workings to be established.

5.3. Implications for shallow mine geothermal

Ground water flow through abandoned mine workings can be considerable; for example, discharge flow rates from the workings of the Shilbottle Seam in Northumberland (UK) ranged from 0.8 ML/d to 2.6 ML/d (median = 1.7 ML/d) (Younger, 2004). If the coal lenses we observed behind pillars are coal lags, then these are indicative of high flow conditions through partially saturated workings. Our work shows that where flow can occur, any collapse, including early spalling of the roof, adds low permeability, clay-rich, lithologies to the system. Within the collapsed breccia, several distinct packages were observed, occasionally showing alteration. The presence of multiple cycles shows that collapse did not occur instantaneously, instead representing a gradual decrease in void space, the migration of the void upwards, and the development of a topography at the base of the seam associated with the sagging and spalling of the roof. During this time flow would still occur, whilst workings are only partially or temporarily flooded, however, fluid pathways would become more tortuous and localised around pillars.

The presence of cycles within the foliated muds suggest that undersaturated fluid flow fluctuated through time in response to changes in groundwater levels, perched mine water, or pulses of hypersaline brines. For deeper workings this could also be triggered by regional groundwater rebound following the end of mining operations (Burke and Younger, 2000). The thickest deposits of foliated muds are in the vicinity of pillars, suggesting that this is the best location for preferential flow pathways after partial collapse of the stall, particularly as collapse in these areas occurs later than the rest of the workings. It is important, however, to consider not only the permeability of the lithologies which make up the mine workings, but also fracture networks which can combine to form flow pathways (e.g. McCay *et al.* 2019). Pillars display increased fracturing compared to the undeformed section (Fig. 6), and the low angle faults which accommodate the final collapse propagate from the pillars into overlying units (Fig. 3). Tectonically deformed coal, which may occur along the edge of pillars (Figs. 3 & 6), has a

significantly reduced permeability (Ju and Li, 2009) which will inhibit flow into stalls. If dewatering triggers collapse following the start of geothermal energy production, natural and collapse related faults may become reactivated (e.g. Bruyn and Bell, 1999; Donnelly, 2006)) leading to damage of the well casing and/or surface subsidence. While large open voids remain, the water capacity and permeability of the flooded workings will remain high; however, after the final stages of collapse (post stage 3/4) the mine will become increasingly less viable as a geothermal reservoir.

After mine abandonment the level of the seam is generally well constrained (Table 1), however, the location, arrangement, and composition of pillar and stalls is often unknown (Bruyn and Bell, 1999). Likewise, the current level of mine water might not reflect the flooding history. This uncertainty is of particular importance for commercial geothermal projects due to the high cost of drilling (Lukawski et al., 2016), with the geothermal potential of a well differing considerably depending on if you intersect a pillar, open stall, or collapsed stall. Where a stall is encountered, the fill type will depend on the stage of collapse and vary considerably along strike (Fig. 3). In general, the presence of a clay-rich collapse breccia will be a sign of at least partial collapse and the presence of shale and sandstone fragments/core with a brick-orange coloration suggests that perched mine waters have developed prior to full saturation of the collapse breccias and may have begun to form low-permeable clay layers. Although the collapse lithologies and clay layers have low permeability, they are also highly plastic and poorly consolidated. During mine dewatering or mine water rebound it is common to observe rapid break outs between sections of the mine (e.g. Wheal Jane abandoned tin mine (Younger, 2002)), suggesting that in some cases collapse may not cause a long term barrier to flow.

We show that the water capacity and permeability of unsaturated pillar and stall workings decreased as the degradation of pillars cause the roof to sag, spall, and eventually collapse. Workings in the final stages of collapse (post stage 3; Fig. 7), have a greatly reduced volume for fluid flow, and an increased number of potential flow pathways into overlying units. When assessing a site for geothermal potential it is therefore essential that the phases of collapse and flooding are considered. The findings presented here will be of use when assessing the potential water capacity of shallow pillar and stall mine workings prior to drilling, or when interpreting borehole information, and combined with site specific factors such as: a) background geology and hydrogeology; b) the

geothermics of the mine, and c) post-mining conditions (Malolepszy, 2003) will inform whether an area is a viable prospect for a mine geothermal energy system.

6 Conclusions

We present for the first time a detailed study of the internal structure of a collapsed pillar and stall coal mine. The internal structure of the workings near Whitley Bay is comprised of eight distinct facies, with lithology, kinematics, stacking patterns and structure consistent with mechanical understanding of mine collapse processes. A five-stage model of stall collapse is proposed, each acting to decrease the overall permeability of the mine. Stage 1 represents the methods used in initial coal extraction, and provides the initial framework for the rest of the collapse. During this time small fragments of coal were deposited on the seam floor. When the seam was abandoned (Stage 2) the size of fragments of coal increased and these were redeposited around pillars during flood events. When the seam was abandoned the roof began to spall (Stage 3), gradually collapsing. At this site there is evidence for multiple events (at least 19 at Whitley Bay), and indications that acid mine water began to form. In Stage 4 it is interpreted that the presence of hypersaline brines led to the cyclical deposition salty muds. Finally (Stage 5), the roof collapses along several normal faults, which led to the subsidence of the overlying stratigraphy. The last section to collapse was closest to the pillar.

We propose that abandoned pillar and stall workings should be considered as a highly heterogeneous, potentially clay-rich, anthropogenic layer developed by varying mechanical and sedimentological processes as collapse progresses. The water capacity and permeability of a collapsing mine will degrade progressively after abandonment as the roof spalls, and finally collapses. While this work is limited to a single unsaturated site, these processes are likely to be widespread and apply to deeper workings prior to final abandonment and flooding. This has significant implications for the shallow mine geothermal sector. Even when a stall is intersected, the stage and style of collapse will affect whether significant flow can be maintained. The well-connected fault and fracture network which overlies the workings could enhance, through increased flow pathways, or degrade, through communication to shallower cool groundwater, the geothermal potential of a site. The sedimentological approach to classifying mine wastes applied at Whitley Bay should provide a useful tool to classify these deposits elsewhere.

516 **References**

517 Alsop, G.I., Marco, S., Weinberger, R., Levi, T., 2016. Sedimentary and structural controls on seismogenic slumping
518 within mass transport deposits from the Dead Sea Basin. Sediment. Geol. 344, 71–90.
519 https://doi.org/10.1016/j.sedgeo.2016.02.019

520 Banks, D., Athresh, A., Al-Habaibeh, A., Burnside, N., 2019. Water from abandoned mines as a heat source:
521 practical experiences of open- and closed-loop strategies, United Kingdom. Sustain. Water Resour. Manag.
522 5, 29–50. https://doi.org/10.1007/s40899-017-0094-7

523 Banks, D., Younger, Paul L, Road, H., Younger, P L, Arnesen, R.-T., Iversen, E.R., Banks, S.B., 1997. Mine-water
524 chemistry: the good, the bad and the ugly. Environ. Geol. 32, 157–174.
525 https://doi.org/https://doi.org/10.1007/s002540050204

526 Bell, F.G., 1986. Location of abandoned workings in coal seams. Bull. Int. Assoc. Eng. Geol. 33, 123–132.
527 https://doi.org/https://doi.org/10.1007/BF02594714

528 Brady, B.H.G., Brown, E.T., 1985. Rock Mechanics for Underground Mining. Chapman and Hall, New York.

529 Bruyn, F.G., Bell, D.I.A., 1999. Subsidence problems due to abandoned pillar workings in coal seams. Bull. Eng.
530 Geol. Environ. 57, 225–237.

531 BSi, 2015. BS 5930 - COP for ground investigations. BSi Standards Ltd.

532 Burke, S.P., Younger, P.L., 2000. Groundwater rebound in the South Yorkshire coalfield: a first approximation
533 using the GRAM model. Q. J. Eng. Geol. Hydrogeol. 33, 149–160. https://doi.org/10.1144/qjegh.33.2.149

534 Carter, P., Jarman, D., Sneddon, M., 1981. Mining Subsidence in Bathgate, a Town Study, in: Gredds, J.D. (Ed.),
535 Proceedings of the Second International Conference on Ground Movements and Structures. Pentech Press,
536 London, Cardiff, pp. 101–124.

537 Chadwick, B.A., Holliday, D.W., Holloway, S., Hulbert, A.G., Lawrence, D.J.D., 1995. The structure and evolution of
538 the Northumberland-Solway Basin and adjacent areas. London:HMSO.

539 Chadwick, R.A., Holliday, D.W., 1991. Deep crustal structure and carboniferous basin development within the
540 iapetus convergence zone, northern England. J. Geol. Soc. London. 148, 41–53.

https://doi.org/10.1144/gsjgs.148.1.0041

Daunton, M.J., 1981. Down the pit: work in the Great Northern and South Wales coalfields, 1870-1914. Econ. Hist. Rev. 34, 578–597.

Dearman, W.R., Money, M.S., Strachan, A.., Coffey, J.R., Marsden, A., 2000. A regional engineering geological map of the Tyne and Wear County, NE England. Bull. Int. Assoc. Eng. Geol. 19, 5–17.

Dochartaigh, B.E.O., 2009. A scoping study into shallow thermogeological resources beneath Glasgow and the surrounding area. Br. Geol. Surv. Res. Rep. IR/09/024, 17pp.

Donnelly, L.J., 2006. A review of coal mining induced fault reactivation in Great Britain. Q. J. Eng. Geol. Hydrogeol. 39, 5–50.

Donnelly, L.J., Culshaw, M.G., Bell, F.G., 2008. Longwall mining-induced fault reactivation and delayed subsidence ground movement in British coalfields. Q. J. Eng. Geol. Hydrogeol. 41, 301–314. https://doi.org/10.1144/1470-9236/07-215

Dunham, K.C., 1983. Ore genesis in the English Pennines: a fluoritic subtype., in: Kisvarsanyu, G., Grant, S., Pratt, W., Koenig, J. (Eds.), International Conference on Mississippi Valley Type Lead-Zinc Deposits. Rolla Press, University of Missouri, pp. 86–112.

Dunham, K.C., 1948. Geology of the Northern Pennine Orefield Volume 1 Tyne to Stainmore. HMSO, London, UK.

Fang, Z., Harrison, J.P., 2002. Numerical analysis of progressive fracture and associated behaviour of mine pillars by use of a local degradation model. Min. Technol. 111, 59–72. https://doi.org/10.1179/mnt.2002.111.1.59

Fielding, C.R., 1985. Coal depositional models and the distinction between alluvial and delta plain environments. Sediment. Geol. 42, 41–48.

Fielding, C.R., 1984a. Upper delta plain lacustrine and fluviolacustrine facies from the Westphalian of the Durham coalfield, NE England. Sedimentology 31, 547–567.

Fielding, C. R., 1984b. A coal depositional model for the Durham Coal Measures of NE England. J. Geol. Soc. London. 141, 919–931.

Fielding, C.R., 1982. Sedimentology and stratigraphy of the Durham coal measures, and comparisons with other

British coalfields. Durham University.

Gabrielsen, R.H., Braathen, A., Kjemperud, M., Valdresbraten, M.L.R., 2016. The geometry and dimensions of fault-core lenses. Geol. Soc. London, Spec. Publ. 439, 1–21. https://doi.org/10.1144/SP439.4

Galloway, R.L., 1898. Annals of Coal Mining and the Coal Trade, Vol 1. ed. London.

Garrard, G.F.., Taylor, R.K., 1988. Collapse mechanisms of shallow coal-mine workings from field measurements. Geol. Soc. London, Eng. Geol. Sprecial Publ. 5, 181–192.

Gee, D., Bateson, L., Sowter, A., Grebby, S., Novellino, A., Cigna, F., Marsh, S., Banton, C., Wyatt, L., 2017. Ground Motion in Areas of Abandoned Mining : Application of the Intermittent SBAS (ISBAS) to the. Geosciences 7, 1–26. https://doi.org/10.3390/geosciences7030085

Godyń, K., 2016. Structurally Altered Hard Coal in the Areas of Tectonic Disturbances – An Initial Attempt at Classification. Arch. Min. Sci. 61, 677–694. https://doi.org/10.1515/amsc-2016-0047

Gray, G., Judd, A.G., 2003. Barium Sulphate Production from Mine Waters in South East, Northumberland. Br. Min. No. 73 North. Mine Res. Soc. Keighley, U.K. NMRS, 72–88.

Hamm, V., Sabet, B.B., 2010. Geothermics Modelling of fluid flow and heat transfer to assess the geothermal potential of a flooded coal mine in Lorraine , France. Geothermics 39, 177–186. https://doi.org/10.1016/j.geothermics.2010.03.004

Healy, P.R., Head, J.M., 1984. Construction over abandoned mine workings. No 34.

Helm, P.R., Davie, C.T., Glendinning, S., 2013. Numerical modelling of shallow abandoned mine working subsidence affecting transport infrastructure. Eng. Geol. 154, 6–19. https://doi.org/10.1016/j.enggeo.2012.12.003

Jackson, I., Lawence, D.J.., Frost, D.V., 1985. Geological notes and local details for Sheet NZ 27 Cramlington, Killingworth and Wide Open (SE Northumberland). Mem. Br. Geol. Surv. Sheets 14.

Jenkins, J.D., 1958. Some Investigations into the Bearing Capacities in the Northumberland and Durham Coalfields. Trans. Inst. Min. Eng. 117, 725–738.

Johnson, G.A.L., 1984. Subsidence and sedimentation in the Northumberland Trough. Proc. Yorksh. Geol. Soc. 45,

71–83.

Ju, Y., Li, X., 2009. New research progress on the ultrastructure of tectonically deformed coals. Prog. Nat. Sci. 19, 1455–1466. https://doi.org/10.1016/j.pnsc.2009.03.013

Kaiser, P.K., Cai, M., 2012. Design of rock support system under rockburst condition. J. Rock Mech. Geotech. Eng. 4, 215–227. https://doi.org/10.3724/sp.j.1235.2012.00215

Karfakis, M.G., Bowman, C.H., Topuz, E., 1996. Characterization of coal-mine refuse as backfilling material. Geotech. Geol. Eng. 14, 129–150.

Keefer, D.K., 1984. Landslides caused by earthquakes. GSA Bull. 95, 406–421. https://doi.org/10.1130/0016-7606(1984)95<406:lcbe>2.0.co;2

Koken, M., Constantinescu, G., 2008. An investigation of the flow and scour mechanisms around isolated spur dikes in a shallow open channel: 1. Conditions corresponding to the initiation of the erosion and deposition process. Water Resour. Res. 44. https://doi.org/10.1029/2007WR006489

Kresse, R., Baudis, U., Jäger, P., Riechers, H.H., Wagner, H., Winkler, J., Wolf, H.U., 2007. Barium and Barium Compounds, in: Ullmann's Encyclopedia of Industrial Chemistry. Wiley-VCH Verlag GmbH & Co. KGaA, Weinheim, Germany. https://doi.org/10.1002/14356007.a03_325.pub2

Labourdette, R., Lascu, I., Mylroie, J., Roth, M., 2007. Process-like modeling of flank-margin caves: from genesis to burial evolution. J. Sediment. Res. 77, 965–979. https://doi.org/10.2110/jsr.2007.086

Lawrence, D.J.., Jackson, I., 1986. Geology of the Ponteland-Morpeth District. Mem. Br. Geol. Surv. Sheets 9 a.

Leeder, M.R., 1974. Lower border group (Tournaisian) fluvio-deltaic sedimentation and palaeogeography of the Northumberland basin, in: Proceedings of the Yorkshire Geological Society. pp. 129–180. https://doi.org/10.1144/pygs.40.2.129

Liu, Y., Lu, C.P., Zhang, H., Wang, H.Y., 2019. Numerical investigation of slip and fracture instability mechanism of coal- rock parting-coal structure (CRCS). J. Struct. Geol. 118, 265–278. https://doi.org/10.1016/j.jsg.2018.11.001

Lokhande, R.D., Prakash, A., Singh, K.B., Singh, K.K.K., 2005. Subsidence control measures in coalmines : A review

64, 323–332.

Loredo, C., Ordóñez, A., Garcia-ordiales, E., Álvarez, R., Roqueñi, N., Cienfuegos, P., 2017. Science of the Total Environment Hydrochemical characterization of a mine water geothermal energy resource in NW Spain. Sci. Total Environ. 576, 59–69. https://doi.org/10.1016/j.scitotenv.2016.10.084

Loucks, R.G., 2007. A Review of Coalesced , Collapsed-Paleocave Systems and Associated Suprastratal Deformation. Acta Carsologica 36, 121–132.

Loucks, R.G., 1999. Paleocave carbonate reservoirs: origins, burial-depth modifications, spatial complexity and reservoir implications. Am. Assoc. Pet. Geol. Bull. 83, 1795–1834.

Loucks, R.G., Mescher, P.K., McMechan, G.A., John, A., Jackson, K.G., Veritas, P.K.M., Drive, P., 2004. Three-dimensional architecture of a coalesced , collapsed- paleocave system in the Lower Ordovician Ellenburger Group , central Texas 5, 545–564. https://doi.org/10.1306/12220303072

Lukawski, M.Z., Silverman, R.L., Tester, J.W., 2016. Uncertainty analysis of geothermal well drilling and completion costs. Geothermics 64, 382–391. https://doi.org/10.1016/j.geothermics.2016.06.017

Malolepszy, Z., 2003. Man-made, low-temprature reservoirs in abandoned workings of underground mines on example of Nowa Ruda coal mine, Poland, in: International Geothermal Conference. Reykjavík, pp. 23–29.

Malolepszy, Z., Demollin-Schneiders, E., Bowers, D., 2005. Potential Use of Geothermal Mine Waters in Europe, in: Proceedings World Geothermal Congress. Antalya, Turkey, pp. 24–29.

Marino, G.G., Gamble, W., 1986. Mine subsidence damage from room and pillar mining in Illinois. Int. J. Min. Geol. Eng. 4, 129–150.

Martin, C.D., Maybee, W.G., 2000. The strength of hard-rock pillars. Int. J. Rock Mech. Min. Sci. 37, 1239–1246. https://doi.org/10.1016/S1365-1609(00)00032-0

McCay, A.T., Shipton, Z.K., Lunn, R.J., Gale, J.F., 2019. Mini thief zones: Subcentimeter sedimentary features enhance fracture connectivity in shales. Am. Assoc. Pet. Geol. Bull. 103, 951–971. https://doi.org/10.1306/0918181610617114

McMechan, G.A., Loucks, R.G., Mescher, P., Zeng, X., 2002. Characterization of a coalesced , collapsed paleocave

reservoir analog using GPR and well-core data 67, 1148–1158.

Menéndez, J., Ordóñez, A., Álvarez, R., Loredo, J., 2019. Energy from closed mines: Underground energy storage and geothermal applications. Renew. Sustain. Energy Rev. 108, 498–512. https://doi.org/10.1016/j.rser.2019.04.007

Miao, X., Ciu, X., Wang, J., Xu, J., 2011. The height of fractured water-conducting zone in undermined rock strata. Eng. Geol. 120, 32–39.

Monaghan, A.A., Dochartaigh, B.O., Fordyce, F., Loveless, S., Entwisle, D., Quinn, M., Smith, K., Ellen, R., Arkley, S., Kearsey, T., Campbell, S.D.., Fellgett, M., Mosca, I., 2017. UKGEOS - Glasgow Geothermal Energy Research Field Site (GGERFS): Initial summary of the geological platform. Br. Geol. Surv. Open Rep. OR/17/006, 205.

Moore, D.G., 1961. Submarine Slumps. J. Sediment. Res. 31, 343–357. https://doi.org/10.1306/74d70b78-2b21-11d7-8648000102c1865d

Murchison, D., Pearson, J., 2000. The anomalous behaviour of properties of seams at the Plessey (M) horizon of the Northumberland and Durham coalfields 79, 865–871.

Mylroie, J.E., Carew, J.L., Moore, A.I., 1995. Blue holes: Definition and genesis. Carbonates and Evaporites 10, 225–233.

Nef, J.., 1965. The Rise of the British Coal Industry, 2nd ed, The British Journal of Psychiatry. Frank Cass & Co. Ltd., Abingdon. https://doi.org/10.1192/bjp.111.479.1009-a

Page, W., 1907. The Victora History of the Counties of England: A History of Durham (Volume 2), Vol 2. ed. Archibald Constable and company limited, London, UK.

Palumbo-Roe, B., Colman, T., 2010. The nature of waste associated with closed mines in England and Wales.

Patsa, L., Zarrouk, S.J., Patsa, E., Van Zyl, D., Arianpoo, N., 2015. Geothermal Energy in Mining Developments: Synergies and Opportunities Throughout a Mine's Operational Life Cycle, Proceedings World Geothermal Congress.

Poulsen, B.A., Shen, B., 2013. Subsidence risk assessment of decommissioned bord-and-pillar collieries. Int. J. Rock Mech. Min. Sci. 60, 312–320. https://doi.org/10.1016/j.ijrmms.2013.01.014

Salamon, M.D.., Ozbay, M.U., Madden, B.J., 1998. Life and design of bord-and-pillar workings affected by pillar scaling. J. South. African Inst. Min. Metall. 89, 135–145.

Salmi, E F, Karakus, M., Nazem, M., 2019. Assessing the e ff ects of rock mass gradual deterioration on the long-term stability of abandoned mine workings and the mechanisms of post-mining subsidence – A case study of Castle Fields mine. Tunn. Undergr. Sp. Technol. 88, 169–185. https://doi.org/10.1016/j.tust.2019.03.007

Salmi, Ebrahim F, Malinowska, A., Hejmanowski, R., 2019. Investigating the post-mining subsidence and the long-term stability of old mining excavations : case of Cow Pasture Limestone Mine , West Midlands, UK. Bull. Eng. Geol. Environ. 1–18.

Sanner, B., 2001. Shallow Geothermal Energy. GHC Bull. June.

Smailes, A.E., 1938. Population Changes in the Colliery Districts of Northumberland and Durham. Geogr. J. 91, 220. https://doi.org/10.2307/1787541

Smails, A.E., 1935. The development of the Northumberland and Durham coalfield. Scott. Geogr. Mag. 51, 201–214. https://doi.org/10.1080/14702543508554344

Stumm, W., Morgan, J.J., 1981. Aquatic chemistry: an introduction emphasizing chemical equilibria in natural waters. John Wiley & Sons, Hoboken, NJ.

Taylor, J.A., Fowell, R.J., 2007. Mining instability and the misuse of the 10-times-seam thickness rule, in: Ribeiro e Sousa, L., Olalla, C., Grossmann, N.F. (Eds.), 11th ISRM Congress. Taylor & Francis Group, London, UK, pp. 63–68.

Turner, B.R., Richardson, D., 2004. Geological controls on the sulphur content of coal seams in the Northumberland Coalfield, Northeast England. Int. J. Coal Geol. 60, 169–196. https://doi.org/10.1016/j.coal.2004.05.003

Wardell, K., Wood, J.C., 1965. Ground instability problems araising from the presence of shallow old mine workings. Proc. Midl. Soc. Soil Mech. Found. Eng. 7, 7–30.

Warren, J.K., 2016. Hypersaline Fluid Evolution During Burial and Uplift, in: Evaporites. Springer International Publishing, pp. 763–832. https://doi.org/10.1007/978-3-319-13512-0_8

691 Watzlaf, G.R., Ackman, T.E., 2006. Underground mine water for heating and cooling using geothermal heat pump
692 systems. Mine Water Environ. 25, 1–14. https://doi.org/10.1007/s10230-006-0103-9

693 Woodcock, N.H., Mort, K., 2008. Classification of fault breccias and related fault rocks. Geol. Mag. 145, 435–440.
694 https://doi.org/10.1017/S0016756808004883

695 Younger, P.L., 2004. Environmental impacts of coal mining and associated wastes: A geochemical perspective.
696 Geol. Soc. Spec. Publ. https://doi.org/10.1144/GSL.SP.2004.236.01.12

697 Younger, P.L., 1998. Coalfield abandonment: geochemical processes and hydrochemical products., in: Nicholson,
698 K. (Ed.), Energy and the Environment-Geochemistry of Fossil, and Renewable Resources. Environmental
699 Geochemistry Series No. 1, Aberdeen (UK), p. 200.

700 Younger, P.L., 1995. Hydrogeochemistry of minewaters flowing from abandoned coal workings in County Durham
701 The Durham minewater study Scope of the study. Q. J. Eng. Geol. Hydrogeol. 28, S101–S113.

702 Younger, P.L., 1994. Minewater pollution; the revenge of Old King Coal. geoscientist 4, 6–8.

703 Younger, P.L., 1993. Possible Environmental Impact of the Closure of Two Collieries in County Durham. Water
704 Environ. J. 7, 521–531. https://doi.org/10.1111/j.1747-6593.1993.tb00881.x

705 Younger, P.L., Banwart, S.A., Hedin, R.S., 2002. Mine water: hydrology, pollution, remediation, Vol. 5. ed. Springer
706 Science & Business Media.

707 Younger, P.L., Sherwood, J.M., 1993. The cost of decommissioning a coalfield: Potential environmental problems
708 in County Durham. Miner. Plan. 57, 26–29.

709 Zhao, Y., Liu, S., Jiang, Y., Wang, K., Huang, Y., 2016. Dynamic Tensile Strength of Coal under Dry and Saturated
710 Conditions. Rock Mech. Rock Eng. 49, 1709–1720. https://doi.org/10.1007/s00603-015-0849-0

711 Zhou, Z., Zang, H., Cao, W., Du, X., Chen, L., Changtao, K., 2019. Risk assessment for the cascading failure of
712 underground pillar sections considering interaction between pillars. Int. J. Rock Mech. Min. Sci. 124, 104142.
713 https://doi.org/https://doi.org/10.1016/j.ijrmms.2019.104142

714 Zhu, W., Chen, L., Zhou, Z., Shen, B., Xu, Y., 2018. Failure Propagation of Pillars and Roof in a Room and Pillar Mine
715 Induced by Longwall Mining in the Lower Seam. Rock Mech. Rock Eng. 52, 1193–1209.

716